Korean Journal of Chemical Engineering
https://doi.org/10.1007/s11814-024-00258-3

ORIGINAL ARTICLE

Experimental Study of Oxy-fuel Combustion and Emission Characteristics Using a 10 kW_{th} Pressurized Fluidized Bed Combustor

Dong-Won Kim[1] · Jong-Min Lee[1] · Gyu-Hwa Lee[1] · Kyoungil Park[1]

Received: 18 June 2024 / Revised: 30 July 2024 / Accepted: 12 August 2024

Abstract

Pressurized oxy-fuel combustion (POFC) is a promising carbon capture and storage technology because of its ability for efficient CO_2 capture and storage at a relatively low cost. However, the experimental studies conducted on this technology considering pressurized conditions are limited compared with those conducted considering atmospheric conditions. Thus, further investigation on the performance and environmental emissions of oxy-fuel combustion is necessary. In this study, oxy-fuel combustion experiments were conducted using a 10 kW_{th} fluidized bed combustion (FBC) test rig at pressures ranging from 3 to 8 bar (g). The effects of combustion pressure, oxygen concentration, and cofiring with different fuels on combustion temperature, unburned carbon, combustion efficiency, as well as SO_x and NO_x emissions were examined. The experimental results showed that the CO_2 concentration in the flue gas exceeds 90% in all POFC scenarios, thus facilitating the carbon capture process. In addition, by increasing the combustion pressure, the unburned carbon and CO concentrations in the fly ash are reduced, thereby improving combustion efficiency. Furthermore, the variations in NO, NO_2, N_2O, and SO_2 emissions were measured to assess their environmental impact. Moreover, cofiring tests using biomass under pressurized oxy-fuel conditions (5 bar (g), 30% O_2:70% CO_2) showed that these conditions are more environmentally sustainable and efficient than other combustion methods for producing energy in a fluidized bed by burning a mixture of coal and biomass.

Keywords Pressurized oxy-fuel combustion · Carbon capture and storage (CCS) · Fluidized bed combustion (FBC) · Combustion efficiency · Environmental emissions

List of Abbreviations

ASU	Air separation unit
CCS	Carbon capture and storage
CFBC	Circulating fluidized bed combustor
CPU	Compression purification unit
FBC	Fluidized bed combustion
FT-IR	Fourier-transform infrared spectroscopy
IDT	Initial deformation temperature
MFC	Mass flow controller
POFC	Pressurized oxy-fuel combustion
UBC	Unburned carbon
U_{mf}	Minimum fluidization velocity

Introduction

Pressurized oxy-fuel combustion (POFC) is a promising CO_2 capture technology because of its ability for high-efficiency CO_2 capture and storage (CSS) at a relatively low cost [1]. A major advantage of POFC is its ability to recover the latent heat of water vapor by subjecting the flue gas to a heat recovery process under pressurized conditions [2, 3]. In addition, when the flue gas is injected into CO_2 purification units (CPUs) and flue gas recirculation fans, the volume of gas entering the system is ~ 80% less than that of air combustion because of the oxy-fuel combustion characteristics. This gas volume reduction decreases the work required for compression, thereby improving the overall combustion efficiency. In addition, operating under pressurized conditions eliminates the risk of air infiltration that can occur under atmospheric pressure conditions, resulting in increased CO_2 purity and reduced compression work in CPUs [4, 5]. Furthermore, the increased density of the flue gas under pressurized conditions enhances the

✉ Kyoungil Park
kyoungil.park@kepco.co.kr

[1] Power Generation & Environment Laboratory, KEPCO Research Institute, 105 Munji-ro, Yuseong-gu, Daejeon, Republic of Korea

Published online: 25 August 2024

heat transfer rate and reduces the equipment size, thereby reducing the construction cost [6, 7].

Current research efforts on POFC are focusing on experimental investigations to validate theoretical models and simulation results [8–11]. These studies aim to optimize the operating conditions, such as combustion pressure, oxygen concentration, and coal particle size, to achieve maximum efficiency and minimal emissions. Experiments conducted using lab-scale pressurized fluidized bed combustors have provided critical insights into the effects of pressure and oxygen concentrations on combustion performance and pollutant formation.

The behavior of sulfur and its enrichment in particulate matter during pressurized combustion is a major research area [12]. Studies have shown that sulfur enrichment in fine particles under certain conditions leads to significant environmental and operational implications. Ongoing research has been focused on the investigation of sulfur transformation mechanisms and the development of strategies to mitigate the adverse effects of sulfur [13, 14].

The optimization of CCS integrated with POFC is another important research area. Various configurations and operational strategies have been investigated to minimize the energy losses associated with CO_2 capture and to enhance the overall plant efficiency. This includes the optimization of air separation units (ASUs) and CPUs to reduce efficiency losses [15].

Despite these advances, the experimental investigation of oxy-fuel combustion under pressurized fluidized bed conditions is limited compared with that under atmospheric pressure conditions. In particular, there is a lack of experimental data on the effects caused by pressure ranges, such as 7–8 bar (g), which are advantageous for the latent heat recovery of flue gas. Herein, we examine the effects of pressure (3–8 bar) and oxygen concentration (21%–35%) on the combustion efficiency and emissions of pollutants (SO_x, NO_x, and N_2O) under air and oxy-fuel combustion conditions using a 10 kW_{th} FBC test rig. In addition, we investigate the impact of biomass cofiring (0%–20%) under pressurized oxy-fuel conditions on combustion performance and the environmental emissions.

Our study provides essential baseline data for the commercialization of the pressurized oxy-fuel fluidized bed combustion (FBC) technology. Experimental data on the combustion characteristics and pollutant emissions under various pressure conditions are crucial in validating and optimizing theoretical models. Furthermore, cofiring experiments using biomass indicate the potential for sustainable fuel utilization, thus contributing to the development of environmentally friendly energy systems. These findings are expected to enhance the economic and environmental efficiency of POFC technology.

Materials and Methods

Experimental Setup

The pressurized fluidized bed test rig shown in Fig. 1 was designed to operate under high temperature and pressure conditions (up to 8 bar (g) and 950 ℃, respectively). This test rig was used to study the interaction between fuel (such as coal) and solid particles (such as bed material and fluidizing sand) within the reactor and to analyze the flue gas and reactivity during the combustion process. The system is composed of four main sections: reaction, monitoring and control integration, electrical supply, and structural sections.

The lower part of the reactor is equipped with a perforated distributor plate to ensure uniform air distribution for smooth fluidization. The basic design concept of this test rig is based on air combustion conditions, but its versatility allows it to be used under various gas combustion conditions. Figure 1a shows the pressure vessel, combustor, windbox, cyclone separator, fuel hopper, screw feeder, gas preheater, reactor zone heater, flue gas cooler, dust collector filter, tar remover, automatic pressure controller, moisture remover, gas supply units (oxygen, carbon dioxide, air), mass flow controllers (MFCs), and various filters.

In the combustor, which is installed within the pressure vessel, entrained solid particles from pressurized combustion are separated using the cyclone separator. After solid particle separation, the gas is fed through the gas cooler, dust collector filter, and tar remover; then it is depressurized to atmospheric pressure and discharged externally. The combustor is equipped with ports, which are used for temperature and pressure measurements. The height and diameter of the reactor are 1.5 m and 0.037 m, respectively. The pressure vessel is used to ensure safety under high temperature and pressure conditions. Fuel was continuously fed into the combustor via the screw feeder, which is controlled by an inverter to adjust its rotation speed for quick and easy fuel injection.

The gas supply system was configured to quantitatively inject air, oxygen, and carbon dioxide through MFCs. Each controlled gas was preheated before being introduced into the reactor. The flue gas or pyrolysis gas exiting the reactor was fed into the cyclone separator and bag filter to collect fine particles and then forwarded to the gas analyzer. A gas sampling port was installed downstream of the pressure control device and connected to the gas analyzer via a heated sampling line capable of maintaining temperatures above 120 ℃. This setup ensured the transfer of the sampled flue gas to the gas analyzer without condensation. The concentrations of flue gas components were analyzed in real time.

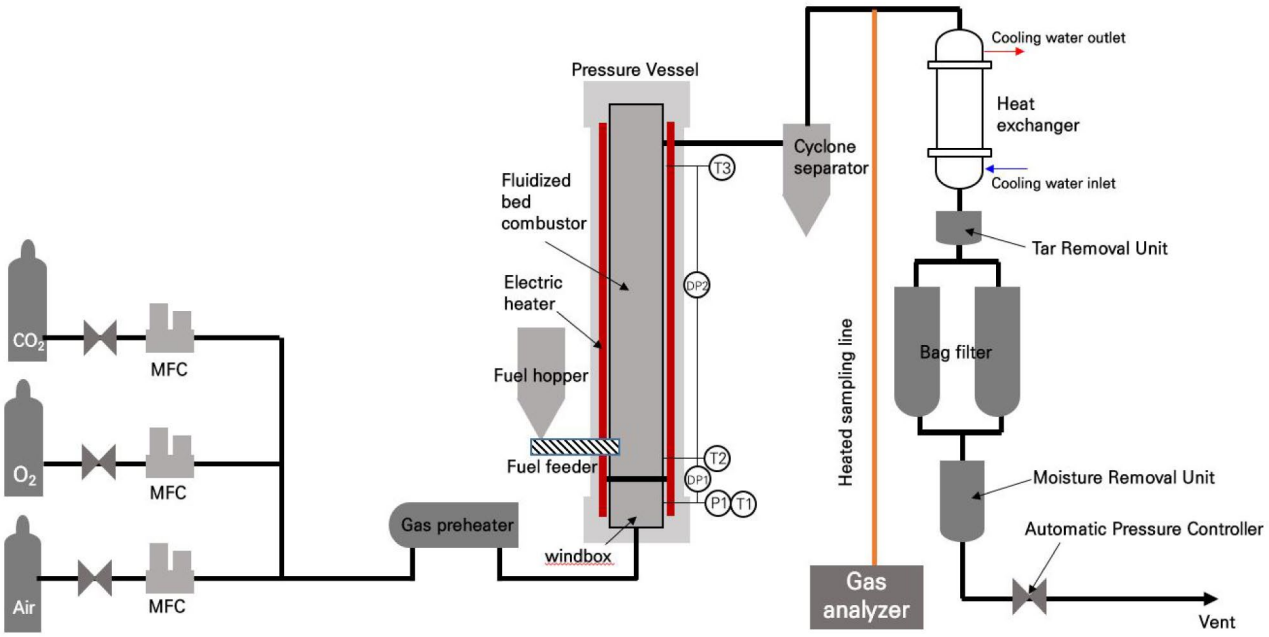

(a) Schematic diagram

(b) Photograph

Fig. 1 **a** Schematic diagram and **b** photograph of the 10kWth pressurized fluidized bed combustor

Table 1 Detailed specifications of gas analyzers

Manufacturer	Types of analyzed gases	Measurement method
Fuji	O_2	Paramagnetic
Gasmet	H_2O, CO_2, CO, NO, NO_2, N_2O, SO_2,	FT-IR[(a)]

FT-IR[(a)] Fourier-transform infrared spectroscopy

In our experiments, we used two gas analyzers: FT-IR gas analyzer (CX4000, Gasmet, Vantaa, Finland) and paramagnetic oxygen analyzer (ZAJ, Fuji Electric, Tokyo, Japan). Detailed specifications are presented in Table 1.

Fuels and Bed Material

In this study, subbituminous coal (obtained from KIDECO Co., Ltd.) and wood pellets were used as fuels. The results of proximate and ultimate analyses as well as heating and initial deformation temperature (IDT) values are presented in Table 2. The particle sizes of the subbituminous coal and wood pellets used were in the 0.85–2.8 mm and 1.4–2.8 mm ranges, respectively. Silica sand (SiO_2) with particle sizes in the 0.85–1 mm range was used as bed material.

Experimental Test Planning

In the combustion test, the system was initially heated to 600 °C using external heaters. After reaching this temperature, the test coal was inserted into the combustor, and the temperature was increased to 850 °C and stabilized for ~ 1 h. Subsequently, combustion and environmental assessments were conducted using measurements obtained over a 30-min period under steady-state conditions. The experimental plan, including variations in reaction pressure, oxygen and carbon dioxide concentrations, and fuel feed rates, is presented in Table 3. The fly ash was collected from the bag filter for analysis.

Results and Discussion

Effect of Operating Pressure Variation on Combustion Performance and Pollutant Formation

The temperature (T2) variation in the lower part of the combustor in the pressurized fluidized bed reactor was measured by varying the operating pressure. As shown in Fig. 2, the temperature in the lower part of the combustor increases with the operating pressure. Table 2 shows that to maintain the fluidization velocity 2.5 times above its minimum value (U_{mf}) despite pressure variation, the flow rate of the reaction gas must be increased proportionally. In addition, to maintain the same excess oxygen ratio, the fuel feed rate must also be increased proportionally. Consequently, the heat input into the combustion reactor was increased, leading to an increase in the lower combustor temperature.

Table 2 Fuel property analysis results

	Subbituminous coal	Wood pellets
Proximate analysis (%) (as received)		
Total moisture	31.16	7.73
Moisture	8.34	6.88
Volatile matter	45.07	78.07
Fixed carbon	40.62	10.61
Ash	5.97	4.44
Sum	100	100
High heating value (kcal/kg, as received)	4357	4250
Ultimate analysis (%) (dry basis)		
C	67.23	49.51
H	4.35	5.54
N	1.01	1.56
S	0.38	0.21
O	20.51	38.37
Ash	6.52	4.81
Sum	100	100
Ash composition (%)		
SiO_2	31.11	34.52
Al_2O_3	9.54	8.97
TiO_2	0.58	1.09
Fe_2O_3	30.86	6.30
CaO	13.62	25.30
MgO	5.40	8.25
Na_2O	1.21	2.49
K_2O	0.80	10.16
SO_3	5.50	0.94
Etc	1.38	1.98
Sum	100	100
IDT (℃)	1208	1210

Furthermore, at the same operating pressure, the combustor temperature under oxy-fuel combustion conditions (hereafter referred to as "oxy 21," representing 21% O_2:79% CO_2) is lower than that under air combustion conditions. This is attributed to the higher specific heat capacity of CO_2 compared with that of N_2, which reduces the combustion temperature, and thus alters the thermodynamic characteristics of the combustion system, as reported in previous studies [6, 8].

Figure 3 shows the variations in O_2, CO_2, and CO concentrations under both air combustion conditions and oxy21 by varying the operating pressure. As the operating pressure

Table 3 Experimental conditions

	Pressure (bar(g))	O_2 (vol %)	CO_2 (vol %)	Coal feeding rate (kg/h)	Wood pellet feeding rate (kg/h)	Total gas flow rate (l/min)
1	3	Air		0.60	–	52.5
2	3	21	79	0.60	–	52.5
3	5	Air		0.90	–	78.8
4	5	21	79	0.90	–	78.8
5	5	30	70	0.90	–	78.8
6	5	30	70	0.81	0.09	78.8
7	5	30	70	0.72	0.18	78.8
8	7	Air		1.17	–	102.4
9	7	21	79	1.17	–	102.4
10	8	Air		1.32	–	116
11	8	21	79	1.32	–	116
12	8	24	76	1.32	–	101
13	8	27	73	1.32	–	90
14	8	30	70	1.32	–	101
15	8	35	65	1.32	–	101

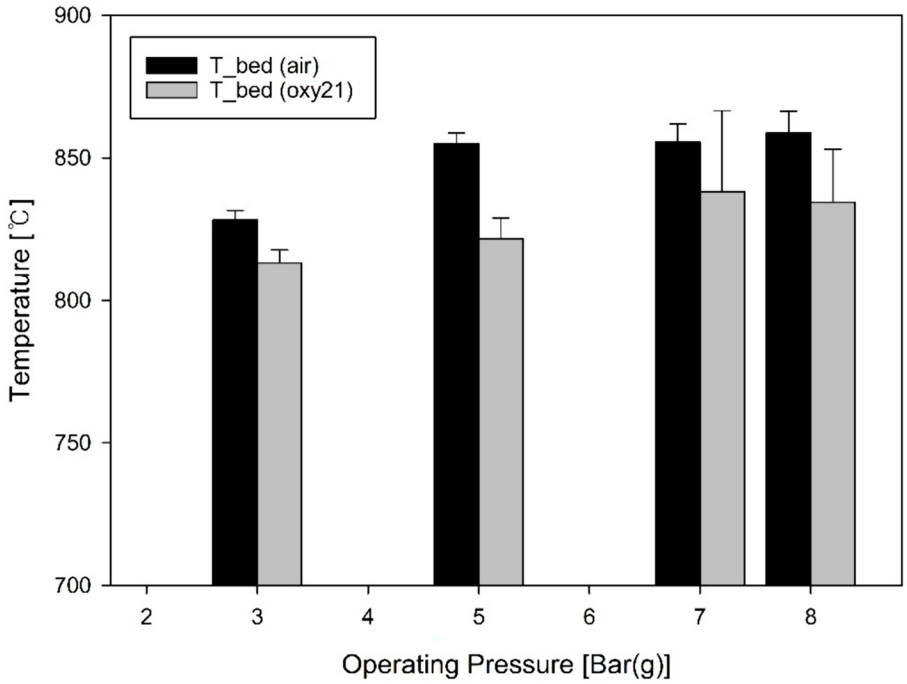

Fig. 2 Bed temperature variation vs. operating pressure

of the oxy-fuel combustion increases, the CO concentration decreases. This is because, according to Le Chatelier's principle, the forward reaction rate of CO oxidation is accelerated at high pressures, and the increased heat input increases the combustion temperature, thus promoting CO oxidation. In addition, as pressure increases, U_{mf} decreases [16]; this, in turn, increases the coal and CO residence times within the reactor, thus providing more time for them to react with oxygen and convert to CO_2.

In contrast, for the same pressure, the CO concentration is generally higher under oxy 21 than that under air combustion conditions. This is attributed to the lower oxygen diffusion coefficient of CO_2 (~ 0.8 times) than that of N_2 and the relatively lower bed temperature under oxy 21 than that under air combustion conditions, as reported in [6]. Furthermore, the higher CO_2 concentration under oxy 21 than that under air combustion conditions enhances the Boudouard reaction, which increases

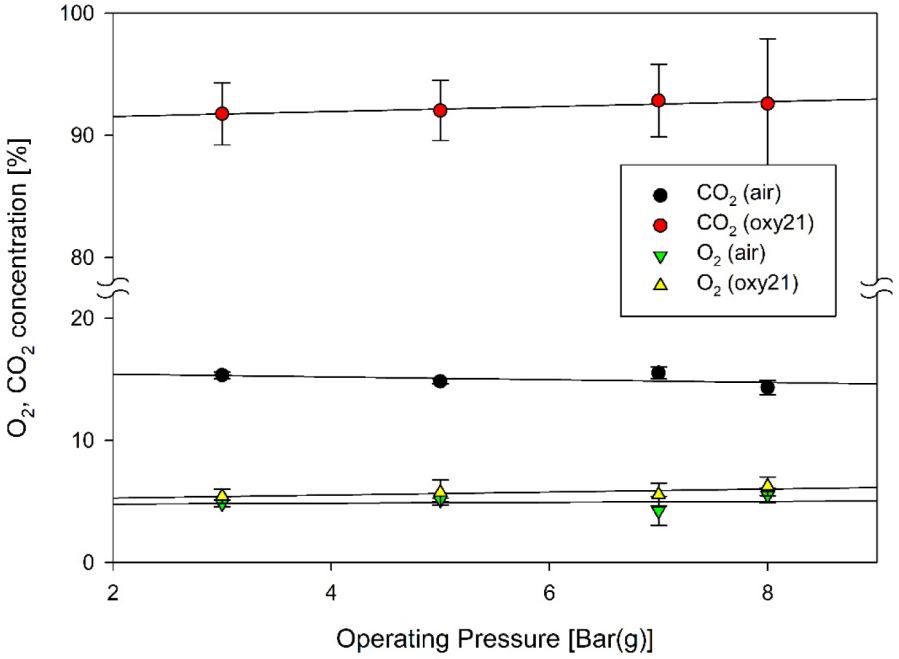

(a) O_2 and CO_2 concentrations

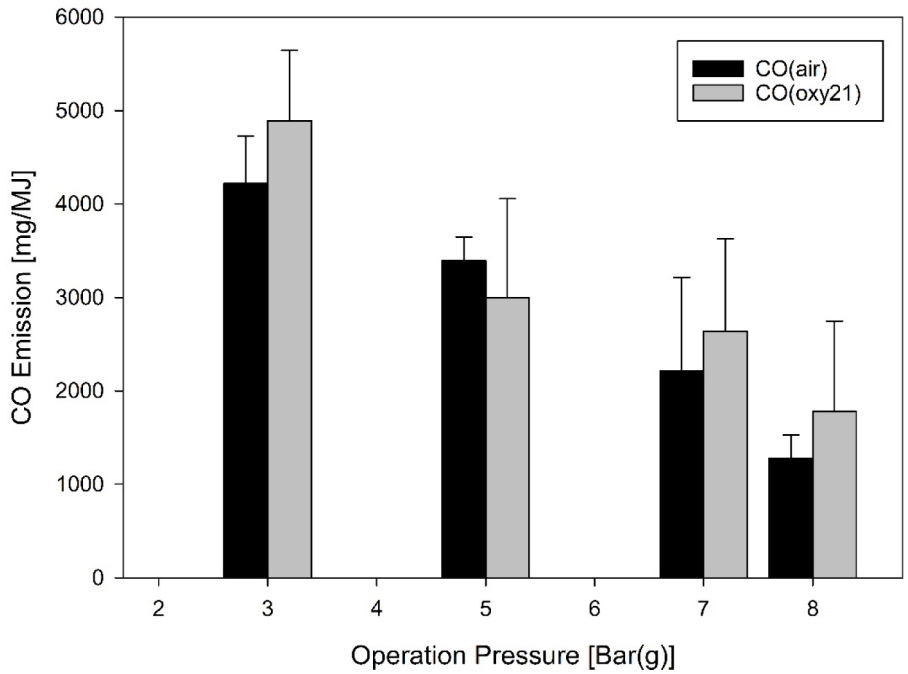

(b) CO emission

Fig. 3 O_2 and CO_2 concentration and CO emission variations vs. operating pressure

the CO concentration. Despite this, for all operating pressures under oxy 21, the CO_2 concentration remains above 90%, which is advantageous in the carbon capture process.

The combustion efficiency is determined by the heat loss due to incomplete combustion, specifically the production of CO and unburned carbon (UBC). Based on this concept, the combustion efficiency can be calculated using the following equation [17, 18]:

$$\text{combustion efficiency (\%)} = 100 \times \left(1 - \frac{\text{heat loss of unburned carbon and CO}}{\text{heat input}}\right) \quad (1)$$

The heat loss due to UBC (MJ/h) can be calculated using the mass of solid particles exiting the reactor (kg/h), the UBC content (shown in Table 4), and the enthalpy of reaction for UBC (MJ/kg). Similarly, the heat loss due to incomplete combustion, which results in CO, can be calculated using the flue gas flow rate (Nm^3/h), the CO fraction in the flue gas, and the enthalpy of reaction for CO (MJ/Nm^3). The heat input from the fuel (MJ/h) can be calculated using the heating value (MJ/kg) and fuel consumption rate (kg/h). The results are shown in Fig. 4.

Table 4 Unburned carbon (UBC) in fly ash under oxy 21

Operating pressure [bar (g)]	3	5	7	8
UBC in fly ash [%]	10.5	9.4	7.5	7.1

As the operating pressure increases, the heat loss attributed to UBC and CO decreases linearly, resulting in an increase in carbon conversion efficiency [18]. At 8 bar (g), the efficiency reaches 98.3%, indicating an improvement of ~ 1.5% compared with that at 3 bar (g).

The variations in the emissions of nitrogen oxides (NO_x) and sulfur oxides (SO_x) by varying the operating pressure are shown in Figs. 5 and 6, respectively. The experimental results show that NO_x in the flue gas mainly consist of NO, NO_2, and N_2O. As the operating pressure increases, NO and N_2O concentrations decrease under both air and oxy-fuel combustion conditions, whereas the NO_2 concentration exhibits an increasing trend.

The decrease in the total NO_x emission by increasing the operating pressure indicates that NO decreases quicker than N_2 through its interaction with char or bed material in the reactor because of its increased residence time; some of it was oxidized to NO_2. It is known that N_2O generally decreases through its interaction with high-temperature radicals, such as O, H, and OH [19, 20]; in this study, it was assumed that the increase in combustion temperature by increasing the operating pressure leads to a proportional decrease in N_2O concentration.

For all operating pressures, NO_x concentrations were higher under oxy 21 than those under air combustion conditions. Previous studies indicated that NO concentration

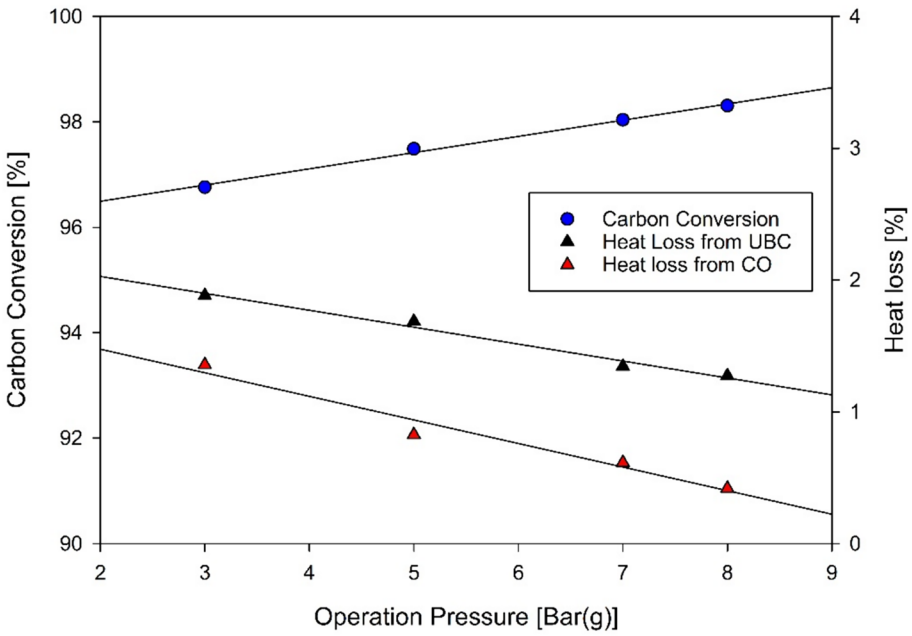

Fig. 4 Carbon conversion vs. operating pressure

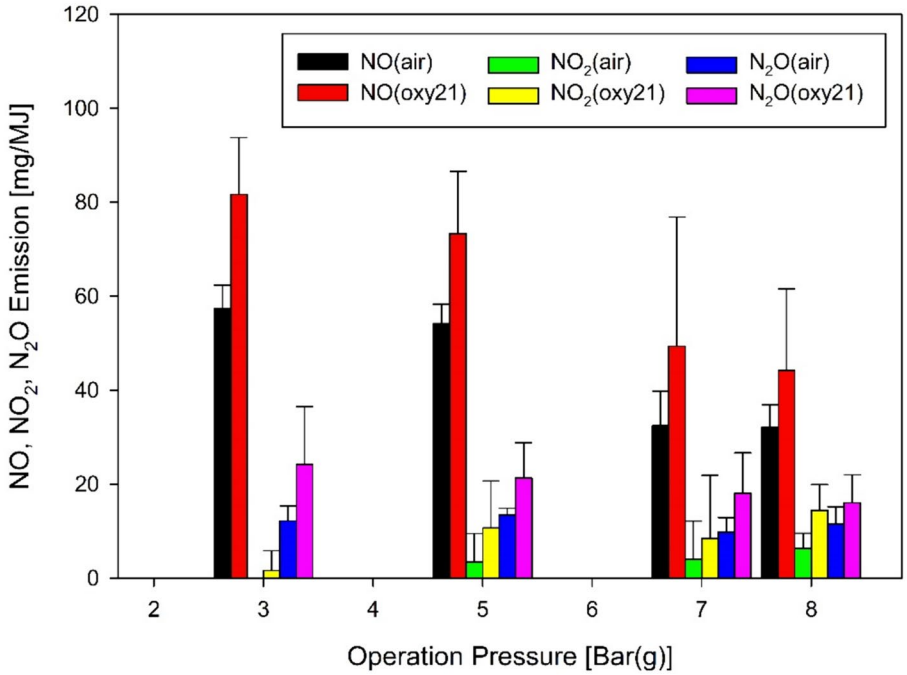

Fig. 5 NO_x emissions vs. operating pressure

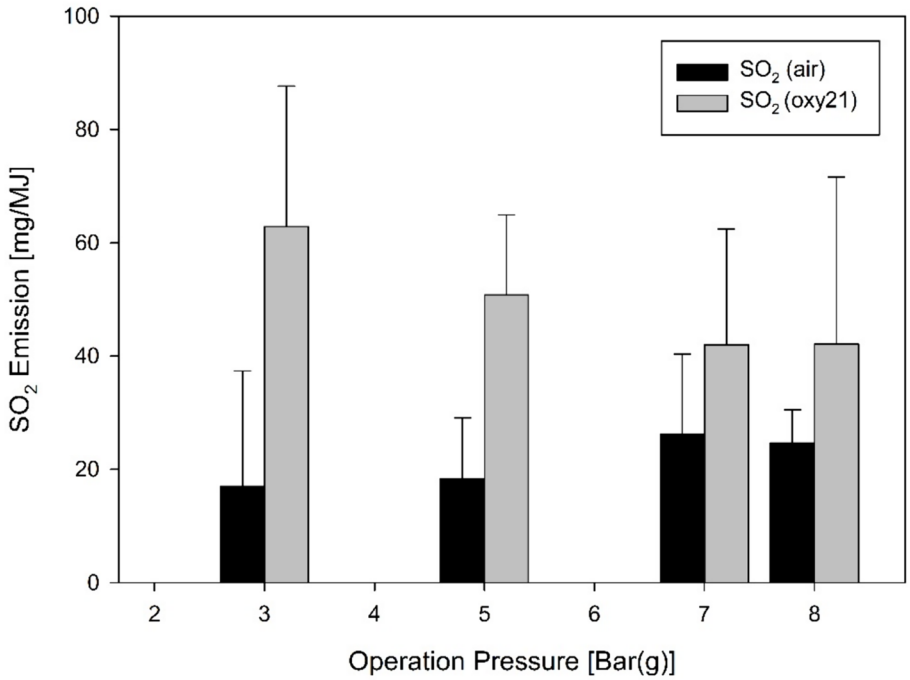

Fig. 6 SO_2 emissions vs. operating pressure

slightly decreases when the combustion mode changes from air to oxy-fuel; however, the opposite trend was observed in this study. This can be attributed to the higher oxygen concentration in the flue gas under oxy 21 than that under air combustion conditions, promoting the oxidation of fuel-bound N_2, as shown in Fig. 5. The relatively higher NO concentration under oxy 21 than that under air combustion conditions probably led to an increase in NO_2 formation.

N_2O concentration increases proportionally at low combustion temperatures under oxy 21, as previously explained. Notably, the proportion of NO_2 in the total NO_x increases from 2 to 25% with the increase in operating pressure (3–8 bar (g)) under oxy 21. Generally, under

air combustion conditions, NO constitutes the majority of NO_x, requiring selective reduction catalysts to reduce NO emissions. However, NO_2 is water soluble and can be easily removed using the direct contact cooler process. This indicates that pressurized oxy-fuel FBC is highly advantageous in the reduction of NO_x emission.

Figure 6 shows the variation in SO_2 emissions with increasing operating pressure under conditions of oxy 21 and air combustion. The coal used in this experiment had a Ca/S molar ratio of 1.8, indicating strong self-desulfurization. Under the conditions of air combustion, $CaCO_3$ in the coal ash is thermally decomposed to form CaO, which reacted with SO_2 in the flue gas to undergo desulfurization. By contrast, under the oxy 21 conditions, high CO_2 content inhibited the thermal decomposition of $CaCO_3$, leading to direct desulfurization by its reaction with SO_2 [13, 21]. The results indicate that pressurized air combustion conditions feature superior desulfurization efficiency than POFC conditions because indirect desulfurization predominantly occurs under pressurized air combustion conditions, whereas under POFC conditions, a relatively higher CO_2 partial pressure inhibiting indirect desulfurization and promoting direct desulfurization exists.

Further investigation revealed that under conditions of air combustion, SO_2 emissions increase with the operating pressure, whereas it decrease under oxy21 conditions. The reason for reduced desulfurization efficiency at high operating pressures under air conditions is the limiting influence of higher CO_2 partial pressures on the thermal decomposition of limestone, which inhibits indirect desulfurization [22]. On the contrary, enhanced desulfurization efficiency with increasing operating pressure under pressurized oxy-fuel conditions is accelerated direct desulfurization.

Effect of Increasing Oxygen Inlet Concentration on Combustion Performance and Pollutant Formation

In pressurized oxy-fuel FBC, two main methods are used to increase the oxygen inlet concentration while keeping the fuel feed rate constant. In the first method, a fixed excess oxygen ratio is maintained by fixing the oxygen flow rate in the reaction gas and reducing the carbon dioxide flow rate, thus increasing the relative oxygen concentration; in this case, the total amount of reaction gas decreases. In the second method, the total amount of reaction gas is maintained by increasing the oxygen flow rate and decreasing the CO_2 flow rate, thus increasing the excess oxygen ratio. In this study, both methods were employed.

Fixed Excess Oxygen Ratio

Figure 7 shows the NO_x concentration and bed temperature variation under excess oxygen ratio conditions (4%) at 8 bar (g) as the oxygen concentration changes. As previously explained, increasing the oxygen inlet concentration reduces the total amount of reaction gas, which, in turn, decreases the internal gas velocity in the reactor. This leads to a decreased expansion of the bubbling fluidized bed, causing combustion to concentrate at the lower bed, thus increasing the lower bed temperature (Fig. 7).

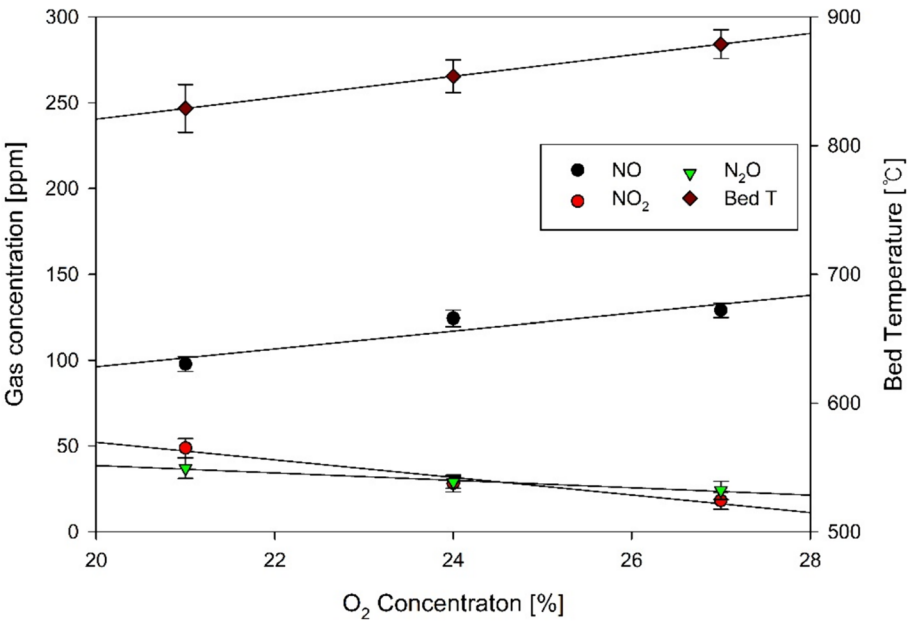

Fig. 7 NO_x concentration and bed temperature variations vs. O_2 concentration (8 bar (g), excess oxygen ratio: 4%)

As the oxygen concentration increases, the NO emission increases due to the increased oxygen partial pressure and residence time in the combustor at high temperatures. Conversely, the NO_2 and N_2O emissions decrease due to enhanced reduction reactions facilitated by the increased combustion temperature and residence time [8].

Fixed Gas Velocity

Figure 8 shows the NO_x concentration and bed temperature variations at 8 bar (g) by varying the oxygen inlet concentration under fixed gas velocity conditions (0.55 m/s). As previously mentioned, increasing the oxygen inlet concentration increases the excess oxygen ratio while maintaining the same internal gas velocity in the reactor. This results in consistent fluidization characteristics and combustion location, leading to stable combustion temperatures (Fig. 8).

The NO concentration increases with the oxygen inlet concentration because of the increase in oxygen partial pressure. However, the N_2O concentration remains almost unchanged because of the consistent combustion temperature. Notably, the increase in NO_2 relative to NO is significant. When the excess oxygen ratio reached 15%, the proportion of NO_2 in the total NO_x increases to 44%. This is because a high oxygen concentration increases the concentration of HO_2 radicals, which promote the conversion of NO to NO_2 [22].

Biomass Cofiring

Figure 9 shows the variations in combustion performance and environmental emissions as a function of the biomass cofiring ratio (0%–20%) under pressurized oxy 30 conditions (5 bar (g), 30% O_2:70% CO_2) at a fixed gas velocity. As shown in Fig. 9, increasing the biomass cofiring ratio leads to a decrease in CO emissions, indicating improved combustion efficiency. Similar to reports that conducted oxy-fuel combustion under atmospheric conditions [23–25], NO_x emissions decrease with an increase in biomass cofiring ratio because of relatively low N_2 content in biomass. In addition, the lower sulfur content in biomass compared with that in coal leads to reduced SO_2 emissions [25].

Under pressurized conditions, the reaction between CaO and SO_2 is enhanced, thus increasing desulfurization efficiency. From a CO_2 capture perspective, biomass cofiring under pressurized conditions increases CO_2 capture efficiency, thus contributing to carbon neutrality or even negative emissions. These results demonstrate that compared with other combustion methods, pressurized oxy-fuel FBC is more environmentally sustainable and efficient in energy production when cofiring coal with biomass.

Conclusion

In this study, the combustion efficiency and emission characteristics of a 10 kW_{th} pressurized fluidized bed combustor were investigated under air and oxy-fuel combustion conditions for various operating pressures (3–8 bar (g)). The following observations can be made by analyzing the experimental results:

1) In all POFC scenarios, the CO_2 concentration in the flue gas exceeded 90%, which is highly advantageous for the

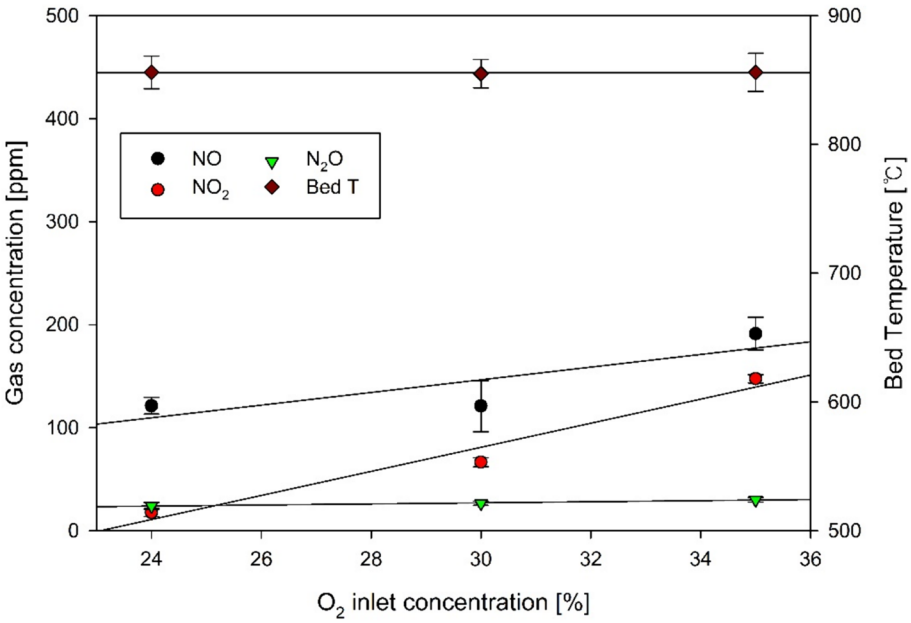

Fig. 8 NO_x concentration and bed temperature variations vs. O_2 inlet concentration (8 bar (g), fixed gas velocity: 0.55 m/s)

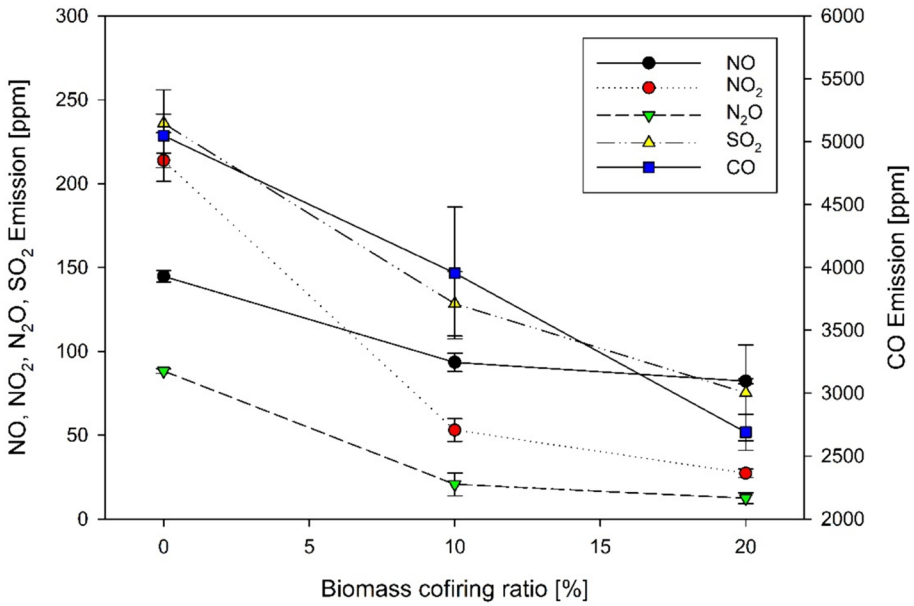

Fig. 9 Variations in combustion performance and environmental emissions vs. biomass cofiring ratio (5 bar (g), 30% O_2:70% CO_2)

carbon capture process. By increasing the combustion pressure, the UBC and CO concentrations in the fly ash were reduced, thereby improving combustion efficiency. At 8 bar (g), the carbon conversion efficiency reached 98.3%, showing an improvement of ~ 1.5% compared to that at 3 bar (g).

2) By increasing the operating pressure, the NO and N_2O concentrations were reduced under both air and oxy-fuel combustion conditions, whereas the NO_2 concentration exhibited an increasing trend. The total NO_x concentration decreased with the operating pressure, indicating that the increased residence time in the combustor and the enhanced interactions with char or bed material led to an increased reduction of NO to N_2. In addition, NO_x emissions were higher under oxy-fuel combustion conditions than those under air combustion conditions; this was probably due to the higher oxygen concentrations in the flue gas, promoting the fuel-bound N_2 oxidation.
3) By increasing the operating pressure, the SO_2 emission concentrations were increased under air combustion conditions, whereas they decreased under oxy-fuel combustion conditions. Under oxy-fuel conditions, the high CO_2 concentration inhibited the thermal decomposition of $CaCO_3$, promoting direct desulfurization where $CaCO_3$ directly reacts with SO_2.

The impact of the two methods used for increasing the inlet oxygen concentration (i.e., maintaining a fixed excess oxygen ratio or a fixed gas velocity) was investigated. In the first method, increasing the oxygen inlet concentration led to reduced total reaction gas volume, which increased NO emissions, whereas the NO_2 and N_2O emissions decreased. In the second method, increasing the oxygen inlet concentration resulted in stable combustion temperatures with a notable increase in NO_2 relative to NO; this was probably due to the increased HO_2 radical concentrations, which promoted the conversion of NO to NO_2.

Finally, under pressurized oxy-fuel conditions (5 bar (g), 30% O_2:70% CO_2), biomass cofiring led to reduced CO emissions, indicating improved combustion efficiency. By increasing the biomass cofiring ratio, NO_x emissions decreased due to the relatively low N_2 content in biomass. In addition, the low sulfur content in biomass led to reduced SO_2 emissions, and the reaction between CaO and SO_2 was enhanced under pressurized conditions, increasing desulfurization efficiency.

In conclusion, the results of this study provide essential baseline data for the commercialization of pressurized oxy-fuel FBC technology. The experimental data on combustion characteristics and pollutant emissions under various pressure conditions are crucial in validating and optimizing theoretical models. Furthermore, the biomass cofiring experiments indicated the potential for sustainable fuel utilization, contributing to the development of environmentally friendly energy systems. These findings demonstrate the environmental and economic benefits of pressurized oxy-fuel FBC technology, paving the way for its broad application in the energy sector.

Acknowledgements The authors would like to thank the Korea Electric Power Corporation (KEPCO) for their financial support and provision of research facilities. Special thanks to our colleagues at the Power Generation & Environment Laboratory for their invaluable assistance and collaboration throughout this study.

Author Contributions Dong Won Kim: Conceptualization, methodology, formal analysis, investigation, writing—original Draft. Jong Min Lee: Software, funding acquisition, supervision, review and editing.

Gyu Hwa Lee: Validation, Investigation, data curation. Kyoung Il Park: Data curation, resources, visualization, project administration, corresponding author.

Funding This work was supported by the Korea Electric Power Corporation (KEPCO) [grant number: R22GJ01].

Data availability Data will be made available upon reasonable request.

Declarations

Conflict of Interest The authors declare that they have no known competing financial interests or personal relationships that could have appeared to influence the work reported in this paper.

References

1. M. Xu, Y. Wu, H. Wu, H. Ouyang, S. Zheng, Q. Lu, Experimental study on oxy-fuel combustion and NO emission in a spouted-fluidized bed. J. Therm. Sci. **30**(4), 1132–1140 (2021). https://doi.org/10.1007/s11630-021-1441-4
2. S. Ajdari, F. Normann, K. Andersson, Evaluation of operating and design parameters of pressurized flue gas systems with integrated removal of NOx and SOx. Energy Fuels **34**(3), 3499–3508 (2020). https://doi.org/10.1021/acs.energyfuels.9b04307
3. J. Hong, R. Field, M. Gazzino, A.F. Ghoniem, Operating pressure dependence of the pressurized oxy-fuel combustion power cycle. Energy **35**(12), 5391–5399 (2010). https://doi.org/10.1016/j.energy.2010.07.026
4. C.K. Stimpson, A. Fry, T. Blanc, D.R. Tree, Line of sight soot volume fraction measurements in air- and oxy-coal flames. Proc. Combust. Instit. **34**(2), 2885–2893 (2013). https://doi.org/10.1016/j.proci.2012.07.009
5. E.H. Chui, A.J. Majeski, M.A. Douglas, Y. Tan, K.V. Thambimuthu, Numerical investigation of oxy-coal burner and combustor design concepts. Energy **29**(9–10), 1285–1296 (2004). https://doi.org/10.1016/j.energy.2004.03.006
6. R. Kong, W. Li, H. Wang, Q. Ren, Energy efficiency analysis of oxy-fuel circulating fluidized bed combustion systems. Energy **286**, 129613 (2024). https://doi.org/10.1016/j.energy.2023.129613
7. M. Xu, J. Yang, L. He, W. Wei, X. Yin, A. Lin, Carbon capture and storage as a strategic reserve against China's CO_2 emissions. Environ. Dev. **37**, 100608 (2021). https://doi.org/10.1016/j.envdev.2020.100608
8. T.F. Wall, J. Yu, C. Spero, L. Elliott, S. Khare, R. Rathnam, F. Zeenathal, B. Moghtaderi, B. Buhre, C. Sheng, R. Gupta, T. Yamada, K. Makino, J. Yu, An overview on oxyfuel coal combustion-state of the art research and technology development. Chem. Eng. Res. Des. **87**(8), 1003–1016 (2009). https://doi.org/10.1016/j.cherd.2009.02.005
9. J. Gu, X. Zhou, M. Xu, H. Wu, 3D simulation on pressurized oxy-fuel combustion of coal in fluidized bed. Adv. Powder Tech. **31**(12), 2792–2805 (2020). https://doi.org/10.1016/j.apt.2020.07.001
10. S. Ajdari, F. Normann, K. Andersson, Towards second generation pulverized coal power plants: energy penalty reduction potential of pressurized oxy-combustion systems. Energy Procedia **63**, 431–439 (2014). https://doi.org/10.1016/j.egypro.2014.11.047
11. X. Liang, Q. Wang, Z. Luo, E. Eddings, T. Ring, S. Li, P. Yu, J. Yan, X. Yang, X. Jia, Experimental and numerical investigation on nitrogen transformation in pressurized oxy-fuel combustion of pulverized coal. J. Clean. Prod. **278**, 123240 (2021). https://doi.org/10.1016/j.jclepro.2020.123240
12. L. Chen, S.Z. Yong, A.F. Ghoniem, Oxy-fuel combustion of pulverized coal: characterization, fundamentals, stabilization and CFD modeling. Prog. Energy Combust. Sci. **38**(2), 156–214 (2012). https://doi.org/10.1016/j.pecs.2011.09.003
13. Y. Duan, L. Duan, J. Wang, E.J. Anthony, Observation of simultaneously low CO, NOx, and SO2 emission during oxy-coal combustion in a pressurized fluidized bed. Fuel **242**, 374–381 (2019). https://doi.org/10.1016/j.fuel.2018.10.134
14. C. Wang, M. Lei, W. Yan, S. Wang, L. Jia, Combustion characteristics and ash formation of pulverized coal under pressurized oxy-fuel conditions. Energy Fuels **25**(10), 4333–4344 (2011). https://doi.org/10.1021/ef200858e
15. H. Zebian, M. Gazzino, A. Mitsos, Multi-variable optimization of pressurized oxy-coal combustion. Energy **38**(1), 37–57 (2012). https://doi.org/10.1016/j.energy.2011.10.023
16. X. Liang, Q. Wang, Z. Luo, E. Eddings, T. Ring, S. Li, J. Lin, S. Xue, L. Han, G. Xie, Experimental and numerical investigation on sulfur transformation in pressurized oxy-fuel combustion of pulverized coal. Appl. Energy **253**, 113542 (2019). https://doi.org/10.1016/j.apenergy.2019.113542
17. Y. Duan, L. Duan, E.J. Anthony, C. Zhao, Nitrogen and sulfur conversion during pressurized pyrolysis under CO_2 atmosphere in fluidized bed. Fuel **189**, 98–106 (2017). https://doi.org/10.1016/j.fuel.2016.11.054
18. D. Kim, K.Y. Huh, Y. Lee, Influence of operating pressure on combustion and heat transfer in pressurized oxy-fuel combustion evaluated by numerical modeling. Int. J. Heat Mass Transf. **201**, 123616 (2023). https://doi.org/10.1016/j.ijheatmasstransfer.2023.123616
19. Y. Duan, C. Zhao, Q. Ren, Z. Wu, X. Chen, NO_x precursors evolution during coal heating process in CO_2 atmosphere. Fuel **90**, 1668–1675 (2011). https://doi.org/10.1016/j.fuel.2010.11.035
20. A. Gopan, B.M. Kumfer, R.L. Axelbaum, Effect of operating pressure and fuel moisture on net plant efficiency of a staged, pressurized oxy-combustion power plant. Int. J. Greenh. Gas Control **39**, 390–396 (2015). https://doi.org/10.1016/j.ijggc.2015.06.012
21. X. Wang, G. Dai, G.S. Yablonsky, M. Vujanović, R.L. Axelbaum, A kinetic evaluation on NO_2 formation in the post-flame region of pressurized oxy-combustion process. Therm. Sci. **24**(6A), 3237–3247 (2020). https://doi.org/10.2298/TSCI200415236W
22. L. Pang, Y. Shao, W. Zhong, H. Liu, Experimental study of SO2 emissions and desulfurization of oxy-coal combustion in a 30 kW_{th} pressurized fluidized bed combustor. Fuel **264**, 116795 (2020). https://doi.org/10.1016/j.fuel.2019.116795
23. S.-S. Hou, C.-Y. Chiang, T.-H. Lin, Oxy-fuel combustion characteristics of pulverized coal under O_2/recirculated flue gas atmospheres. Appl. Sci. **10**(4), 1362 (2020). https://doi.org/10.3390/app10041362
24. Y.R. Gwak, J.H. Yun, S.I. Keel, S.H. Lee, Numerical study of oxy-fuel combustion behaviors in a 2MWe CFB boiler. Korean J. Chem. Eng. **37**, 1878–1887 (2020). https://doi.org/10.1007/s11814-020-0611-5
25. H.K. Nguyen, J.-H. Moon, S.-H. Jo, S.J. Park, M.W. Seo, H.W. Ra, S.-J. Yoon, S.-M. Yoon, B. Song, U. Lee, C.W. Yang, T.-Y. Mun, J.-G. Lee, Oxy-combustion characteristics as a function of oxygen concentration and biomass co-firing ratio in a 0.1 MWth circulating fluidized bed combustion test-rig. Energy **196**, 117020 (2020). https://doi.org/10.1016/j.energy.2020.117020